Chemistry and Physics of Lipids 267 (2025) 105464

Contents lists available at ScienceDirect

Chemistry and Physics of Lipids

journal homepage: www.elsevier.com/locate/chemphyslip

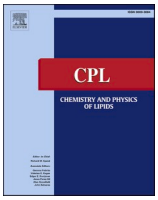

Effect of hydrophobic proteins in modulating the mechanical properties of lung surfactant membranes

Ainhoa Collada [a,b], Johann Mertens [c,*], Emma Batllori-Badia [d], Alberto Galindo [b,d,e], Antonio Cruz [a,b,**], Jesús Pérez-Gil [a,b]

[a] Biochemistry and Molecular Biology Department, Faculty of Biology, Complutense University, Madrid, Spain
[b] Research Institute Hospital 12 de Octubre (imas12), Madrid, Spain
[c] Institute for Advanced Studies in Nanoscience (IMDEA Nanoscience), Campus Cantoblanco, Madrid 28049, Spain
[d] Department of Public and Maternal-Child Health. Faculty of Medicine, Complutense University of Madrid. 12 de Octubre University Hospital, Spain
[e] Maternal and Child Health and Development Research Network (RICORS-SAMID Network), Spain

ARTICLE INFO

Keywords:
Surfactant proteins
Membrane mechanics
Surface tension
Air-liquid interface
Membrane thickness

ABSTRACT

Pulmonary surfactant is a membranous complex that enables breathing dynamics at the respiratory surface. Extremely low values of surface tension are achieved at end-expiration thanks to a unique mixture of lipids and proteins. In particular, the hydrophobic surfactant proteins, specially the protein SP-B, are crucial for surfactant biophysical function, in order to provide the surfactant lipid matrix with the ability to form membranous multi-layered interfacial films that sustain optimal mechanical properties. To analyse the contribution of the proteins to modulate the resistance to mechanical forces of surfactant membrane-based structures, atomic force microscopy of supported lipid bilayers has been used here to determine quantitative mechanical parameters defining the effect of the presence of proteins SP-B and/or SP-C on phospholipid membranes intended to model at least part of the structures integrated into pulmonary surfactant complexes. The results show clear differences introduced by proteins in membrane thickness, lateral packing and elasticity, providing evidence supporting protein-promoted modulating of the mechanical properties of surfactant membranes. These effects are found consistent with the behaviour of two relevant native materials: whole pulmonary surfactant isolated from porcine bronchoalveolar lavages and freshly produced human pulmonary surfactant isolated from amniotic fluid, where it is transferred from the foetal lung before the respiratory air-liquid interface has been established.

1. Introduction

In mammalian lungs, a thin lipid-based layer coats the alveolar surface and provides the alveoli with the reduction of surface tension needed to perform breathing cycles without collapsing (Pérez-Gil, 2008). This material, known as pulmonary surfactant (PS), is required for a correct performance of breathing dynamics with minimal work and its dysfunction is associated to severe respiratory pathologies (Echaide et al., 2017). Surfactant composition (90 % of its total mass are lipids, mainly phospholipids, and less than 10 % are proteins) provides it with the ability of rapidly coating the alveolar interface during inspiration and efficiently re-spread during expiration thanks to the action of two specific hydrophobic proteins, SP-B and SP-C, that generate membrane curvature and membrane/membrane contacts to keep previously excluded material and newly synthesised surfactant in close contact with the interfacial film for its use when needed (Haller et al., 2004; Veldhuizen et al., 1998).

With regard to the lipids, DPPC is the major component (40 %, mass) of surfactant and the only one able to sustain the extreme reduction in surface tension needed to stabilize the alveoli during expiration thanks to its disaturated structure (Veldhuizen et al., 1998). Other lipid and protein components are needed to modulate its properties and facilitate the transit of DPPC-rich complexes towards the interface (Yu and Possmayer, 2003).

Hydrophobic surfactant proteins, accounting for less than 1 % of total surfactant weight, strongly interact with phospholipids, playing critical roles in the formation and stabilization of surfactant films (Lopez-Rodriguez and Pérez-Gil, 2014). Protein SP-B (8.7 kDa) has an

* Corresponding author.
** Correspondence to: Dept. of Biochemistry and Molecular Biology, Faculty of Biology, Complutense University, José Antonio Novais 12, Madrid 28040, Spain.
E-mail addresses: johann.mertens@imdea.org (J. Mertens), acruz@ucm.es (A. Cruz).

https://doi.org/10.1016/j.chemphyslip.2024.105464
Received 8 November 2024; Received in revised form 8 December 2024; Accepted 17 December 2024
Available online 21 December 2024

amphipathic α-helical structure that remains permanently associated to surfactant membranes. Its lack is lethal, illustrating its crucial role in the stabilization of an open respiratory surface (Melton et al., 2003). Through its net positive charge, SP-B is able to establish electrostatic interactions with anionic phospholipids, leading to a peripheral disposition within the membrane plane. SP-B oligomerizes, deforming the membranes to create a sort of lipid channel that facilitate a rapid traffic of lipids from one membrane to another and to the interfacial monolayer stabilizing the interface (Olmeda et al., 2015; Baoukina and Tieleman, 2011). It has also been described that SP-B can induce aggregation of liposomes and fusion of membranes in vitro (Baoukina and Tieleman, 2010; Keating et al., 2012).

SP-C (3.7 kDa) is a very hydrophobic polypeptide that inserts into membranes in the form of a hydrophobic transmembrane α-helix. SP-C maintains its positively charged N-terminal region also anchored to the bilayer thanks to the post-traslational modification of two cysteines by two palmitic chains, allowing it to slightly tilt in order to fit into the membrane, adapting to different thicknesses and curvatures until it is excluded from the interface when surfactant films are compressed to high pressures, as it occurs at the end of expiration (Roldan et al., 2015; Plasencia et al., 2008). It also interacts with anionic phospholipids (Takamoto et al., 2001) and with SP-B (Cabré et al., 2018), suggesting that at least in part of surfactant actions SP-B and SP-C may act in a concerted manner.

Although their molecular mechanism is still to be described in detail, it is known that SP-C together with SP-B are responsible for the formation of fluid lipid-enriched multilayers upon compression of the respiratory interface, closely attached to the interfacial PS monolayer. These structures have been demonstrated to be crucial to ensure mechanical stability of PS films during breathing dynamics (Pérez-Gil, 2008; Parra et al., 2011).

A proper function of the pulmonary surfactant system is essential to sustain operational breathing, and its lack or deactivation is associated with severe pathologies. This is the case of the very premature neonates, born before their lungs have matured to produce surfactant, which are currently treated as soon as possible after birth by endotracheal administration of an exogenous surfactant material (Echaide et al., 2017). Until nowadays, the materials used for clinical treatment are mainly obtained from animal lungs, as they exhibit similar composition, structure and function than human surfactant complexes (Pfister et al., 2009; Singh et al., 2015). The recent isolation and characterization of a surfactant purified from human amniotic fluid (AFS, amniotic fluid surfactant) (Castillo-Sánchez et al., 2022) has revisited historic work that used this material to treat premature babies (Hallman et al., 1983, 1976). It is a material easily isolated from a human source that could retain the characteristics of a surfactant newly synthesised but still unexposed to the air-liquid interface, not degraded or inactivated as a consequence of the exposure to the demanding environmental conditions of aerated lungs, and fully active. It has been reported that this surfactant may still preserve the highly packed and dehydrated state in which it was originally assembled, stored and secreted by the lamellar bodies of the type II pneumocytes (Castillo-Sánchez et al., 2022; Lemke et al., 2017). To what extent such highly packed state is important for the optimal mechanical properties of the films primarily formed at the respiratory surface has not been determined.

The aim of this study was to further analyse the effect of the presence of proteins SP-B and SP-C to modulate the mechanical properties of bilayers of different nature in response to mechanical deformation by means of Atomic Force Microscopy (AFM). We have compared the behaviour under the AFM of membranes made of a mixture of major surfactant lipids (DPPC, POPC, POPG) and hydrophobic proteins (SP-B and/or SP-C) with that of natural surfactant membranes. We proceeded systematically varying membrane composition in order to probe the contribution of different relevant lipids, and incorporating proteins. We have shown the presence of multi-layered structures and measured the local elasticity of these membrane-based films formed onto mica surfaces. We also recognize features defined by the presence of the hydrophobic proteins SP-B and SP-C in the natural lipid systems, which could be important to modulate the mechanical properties of the films as they may work in vivo at the respiratory surface.

2. Materials and methods

2.1. Materials

Lipids were bought from Avanti Polar Lipids (Alabaster, AL, USA), dissolved in chloroform/methanol (2:1 v:v), both solvents from Sigma Aldrich (Saint Louis MO, USA), and stored at −20°C. Protein stocks were derived from an organic extraction of porcine surfactant and were purified in organic solvents by two subsequent exclusion chromatographies in LH-20 and LH-60 resins (Pharmacia, Sweden) as described elsewhere (Pérez-Gil et al., 1993). After purification, they were also preserved at −20°C.

The different materials were typically suspended or diluted to the operational concentrations in Tris-NaCl buffer (5 mM Tris, 150 mM NaCl, pH=7).

2.2. Methods

2.2.1. Sample preparation

For synthetic samples, small unilamellar vesicles (SUVs) were prepared by extrusion from MLVs. The proper quantities of lipids and proteins to obtain a mixture roughly mimicking pulmonary surfactant with a simplified composition of DPPC/POPC/POPG (50:25:15 w:w:w), named as LM from now on, with or without 10 % by weight of SP-B and/or SP-C were dried under a N_2 stream and 2 h of vacuum centrifuge. Then, the dry films obtained were resuspended in the proper amount of buffer to obtain a final concentration of 100 μg/ml and subjected to hydration in a Thermomixer (Eppendorf; Hamburg, DE) upon incubation at 45 °C 1 h with intermittent shaking. The MLVs obtained were then extruded through 50 nm polycarbonate membranes, producing a relatively homogeneous suspension of SUVs of 50 nm of diameter.

Native surfactant (NS) was purified from bronchoalveolar lavages of porcine lungs as described previously (Taeusch et al., 2005). Amniotic Fluid was obtained from programmed caesareans at term pregnancy (upon informed consent signed by donor mothers) as approved by the Ethical Committee of Hospital 12 de Octubre (Madrid, Spain) in collaboration with its Obstetrics and Gynaecology Service. Amniotic fluid surfactant (AFS) was purified following a similar procedure to that of NS (Castillo-Sánchez et al., 2022; Taeusch et al., 2005). Both, NS and AFS, contain not only the hydrophobic but also the hydrophilic membrane-associated surfactant protein SP-A.

Both, NS and AFS were diluted to a concentration of 100 μg/ml in buffer solution prior to their deposition onto the mica surfaces.

2.2.2. Atomic force microscopy

20 μl of each lipid or lipid/protein preparation were deposited onto freshly exfoliated mica (Electron Microscopy Science, Munich, Germany), and incubated for 10 minutes before measuring. The mica substrate with deposited sample was then placed in a homemade liquid chamber. Measurements were performed both at room (20 °C) and at physiological temperature (37 °C) in aqueous solutions by using a Peltier device at the base on which the samples were attached. The same Tris-NaCl buffer used to prepare the samples was used to create the liquid atmosphere.

The mica-supported lipid membranes were repeatedly imaged with a commercial Nanotec Cervantes AFM (Nanotec, Madrid, Spain) operated under jumping mode (JM-AFM), in which the force between the tip of the cantilever and the probe is kept constant and controlled using an electronic feedback loop after each interaction point during imaging. We used RC800PSA Olympus silicon nitride cantilevers (Olympus, Tokyo, Japan) with a 0.1 N/m nominal force constant, < 20 nm tip radius

(15 nm typical) and 18 kHz nominal resonance frequency. The spring constant for the cantilever was calibrated before each experiment by Sader's method. The settings used were: Imaging 128 × 128 points, applied force: 200 pN; speed: 0.428 line/s. Prior to imaging, the applied force was first calibrated by single Force vs. Z-piezo displacement curves (FZ) on the freshly cleaved mica surface prior to lipid deposition.

To investigate quantitatively the elastic response of the lipid and lipid-protein membranes, we recorded single *FZ* curves in which the applied force was obtained as a function of the displacement of the *Z*-piezo upon which the sample was mounted. A series of 10–20 successive *FZ* curves, each one every 5 s, were performed on the regions of the sample formed by SLBs at a loading rate of 50 nm/s and a maximal force of 0.5 nN, after which the membrane was reimaged, and its height was measured. Measurements were performed on several areas of the same membrane to obtain 100–200 indentations for each sample. No force was observed until the tip contacted the membrane. The nano-indentation process was almost completely reversible. Determination of specific parameters, such as bilayer thickness, was performed specifically in regions of the images with only SLBs, avoiding where some three-dimensional structures appeared in the presence of the proteins.

The elastic modulus is usually estimated from the slope of the curve that displays membrane deformation. Membrane Young's modulus can thus be modeled by using the Sneddon's equation for conic indenter (Sneddon, 1948). Sneddon's model assumes that indentation is occurring into an infinite half-space of homogeneous material (which is not the case for SLBs where the substrate may affect the measurements when the indentation depth is close to the bilayer height). Another limitation is that Sneddon's equation does not take into account adhesion forces during tip retraction (backward curve). For these reasons, even if we indented up to 6 nm, we only fitted the first 2 nm of each curve to discard the undesirable effect of the hard mica support on the curve shape. The spring constant for the cantilever was determined by calibration on the substrate. For soft biological samples, the Poisson's ratio is generally set to 0.5 as for incompressible materials. This parameter and its distribution informs about the tendency of a given material to expand in directions perpendicular to the direction of compression. We applied the Sneddon's fit to every force curve to obtain a histogram that shows the number of events for the Young's modulus of a sample at a fixed temperature. To each of these histograms, a Gaussian fit is adjusted and then the maximum value of the Gaussian curve that fits best to the histogram is selected. All results are expressed as mean ± standard deviation. Statistics were performed via unpaired Student's *t*-test being values of $P < 0.05$ considered as significant.

Image analyses were performed with the help of the WsXM software (Horcas et al., 2007). Each image was individually treated using local plan fit and "flatten plus" that provide filter to eliminate slopes, low frequency noise and shadowing effects. Nanoindentation analysis was performed using AtomicJ program (Hermanowicz et al., 2014). Data analysis and representation was performed with Origin 8.5 (www.origin.com).

3. Results

For the nanomechanical characterization under AFM, the sample is generally first imaged and then a series of force-distance curves is recorded over the same area. We took cross sections of the topography to evaluate the thickness of the phospholipid layers deposited. In each force-distance curve, the AFM tip away from the surface is approached and retracted at constant velocity while the cantilever deflection is recorded as a function of the Z piezo position.

3.1. Topographic images

The measured thickness of pure lipid mix (LM) bilayers composed of DPPC/POPC/POPG (50:25:15 w:w:w) is given in Fig. 1 and has values of 5.63 ± 0.12 nm at 20 °C and 5.34 ± 0.16 nm at 37 °C. The surfaces of the bilayers were relatively flat (Fig. 2A) with lateral sizes of the extended membranes of about 100 nm under our deposition conditions (see

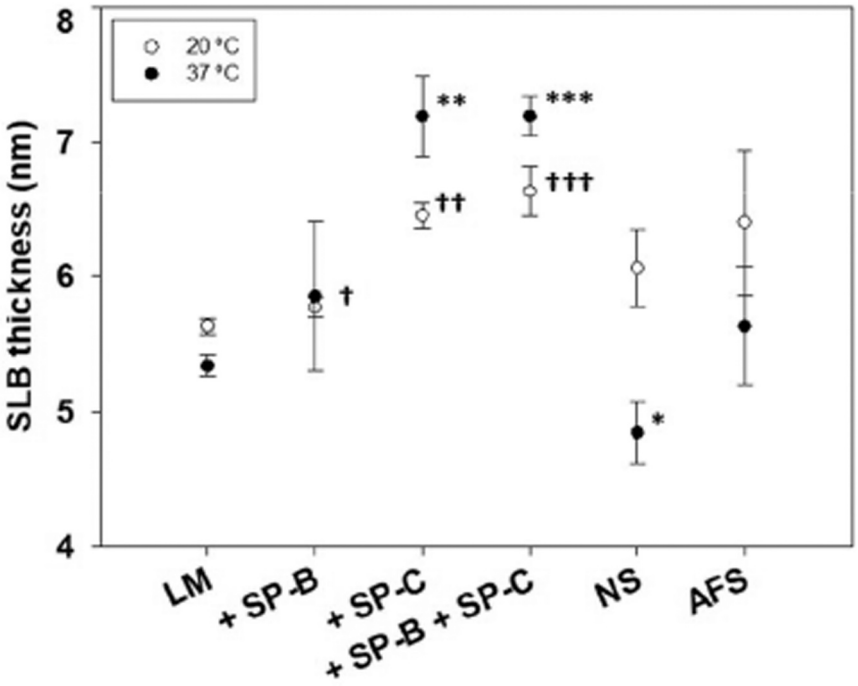

Fig. 1.. Thickness of supported lipid bilayers calculated from cross-sectional analyses of the AFM topographical images at 20 and 37 °C. The values show large differences with increasing uncertainty (standard deviation from the average) when incorporating the proteins SP-B and SP-C to the Lipid Mix composed of DPPC/POPC/POPG (50:25:15, w:w:w), which is confirmed with measurements on layers made of the whole natural systems: native surfactant (NS) and amniotic fluid surfactant (AFS). Significant *p*-values are depicted as daggers for 20 °C (†, $p < 0.05$; ††, $p < 0.005$; †††, $p < 0.0005$) and asterisks for 37 °C (*, $p < 0.05$; **, $p < 0.005$; ***, $p < 0.0005$).

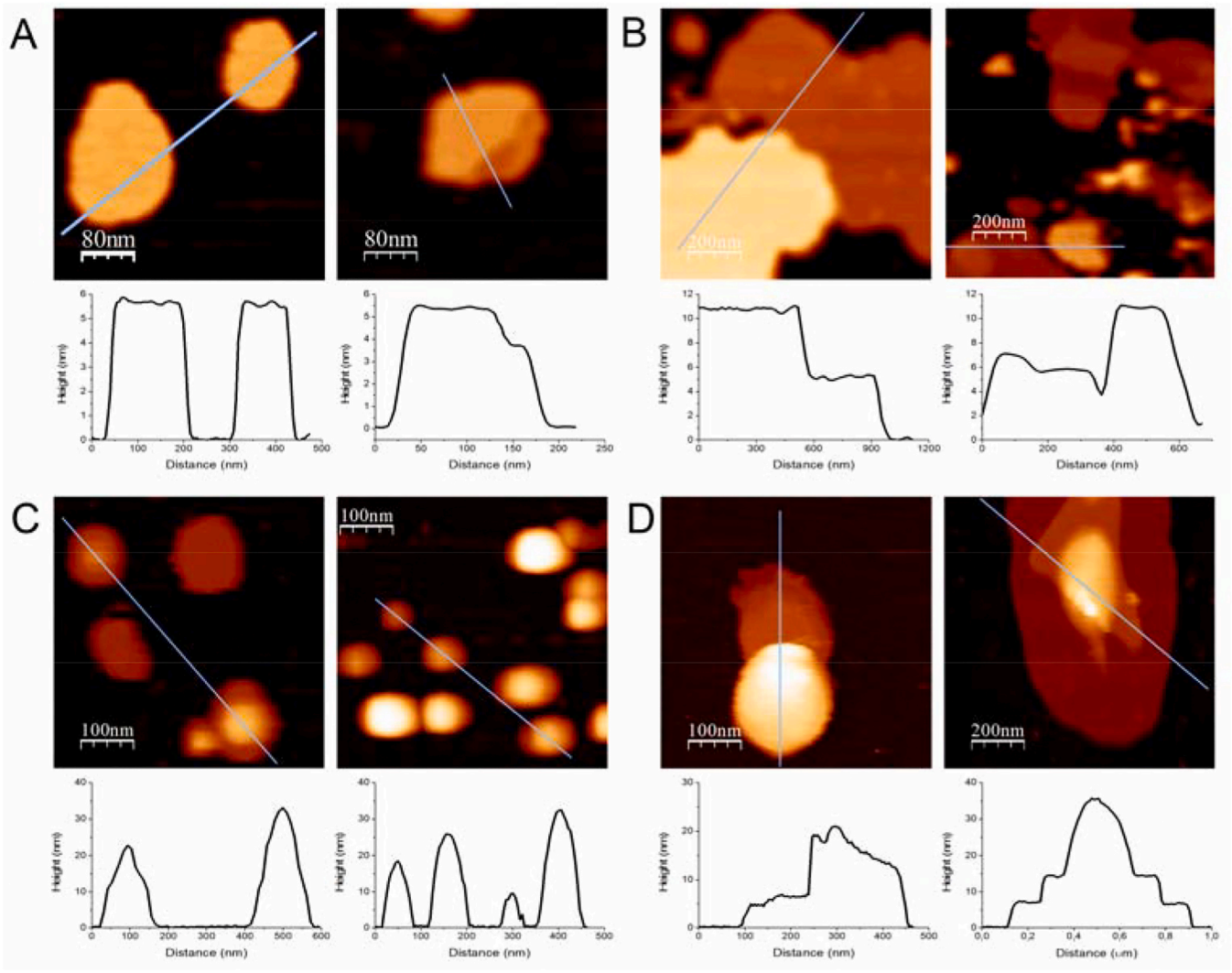

Fig. 2. Topographic AFM images of LM membranes analysed in the absence or presence of surfactant proteins. Images were obtained at both 20 °C (left) and 37 °C (right) of (A) DPPC/POPC/POPG (50:25:15 w:w:w) (400 ×400 nm^2, Z-scale: 10 nm), (B) DPPC/POPC/POPG with 10 % of SP-B (1 ×1 μm^2, Z-scale: 15 nm), (C) DPPC/POPC/POPG with 10 % SP-C (500 ×500 nm^2, Z-scale: 50 nm), and (D) DPPC/POPC/POPG with both 10 % of SP-B and 10 % of SP-C (500 ×500 nm^2, Z-scale: 20 nm). The lines indicate the cross section profiles shown at the bottom of each image.

methods). Different lipid phases can be observed at the temperature of 37 °C, as shown in the height profiles, being the height differences associated with a difference in the mechanical properties of the films.

With the incorporation of SP-B into the lipid mixture, the size of the membranes coating the mica support increased up to bilayers of 500 nm of diameter, illustrating that SP-B somehow favours lateral spreading of the bilayers (Fig. 2B). Moreover, the presence of SP-B induced the formation of multi-layered structures, with the protein prompting membrane contacts and thus, aggregation. Interestingly, we didn't observe the formation of more than two stacked bilayers at the surface of the mica. That means that the lipids added at the top of the two bilayers are more likely to glide or fuse to the previously stacked bilayers than extending it. Bilayer thickness in the presence of SP-B was measured to be 5.77 ± 0.15 at 20 °C and 5.85 ± 1.1 nm at 37 °C (Fig. 1), 5 % more than measured in LM membranes.

With the addition of SP-C to the lipid mixture, the system forms flat 100 nm-size bilayers (Fig. 2C), with many vesicles remaining as not fully extended, much more numerous than observed in any of the other samples studied. Also, the apparent vesicle diameter decreases, with an apparent medium height of 23.1 ± 0.8 nm at 20 °C and 13.6 ± 0.9 nm at 37 °C (Fig. 3). Therefore, that means that the presence of SP-C promotes the stability of the spherical shape of the vesicles, revealed by the

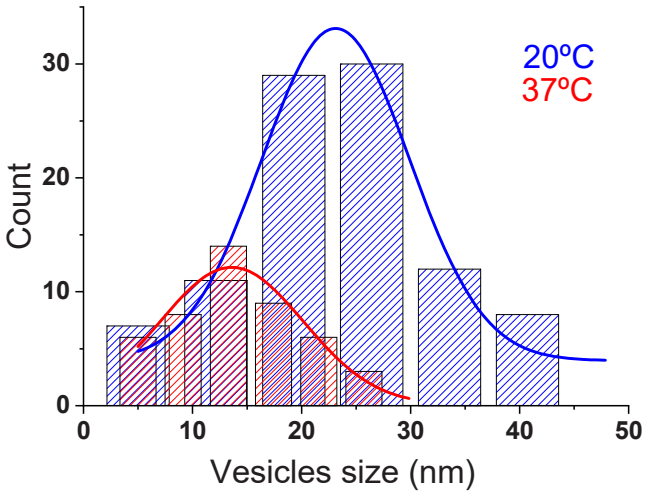

Fig. 3. Vesicle diameter measured for samples containing protein SP-C. Diameter of vesicles found in samples of DPPC/POPC/POPG (50:25:15 w:w:w) + 10 % SP-C attached to the mica surface before forming SLBs.

AFM topographic profile, probably affecting lipid spreadability. This rounding feature likely prevents the membrane to spread and extend. The thickness of the SP-C-containing bilayers was measured to be 6.45 ± 0.19 nm at 20 °C and 7.2 ± 0.6 nm at 37 °C (Fig. 1), 18 % and 34 % more than LM membranes respectively. This large and significant difference suggests a release in the surface tension between bilayer leaflets as generated by SP-C incorporation.

The incorporation of both SP-B and SP-C to the lipid mixture, originated larger and several flat multi-layered membrane stacks with some large, rounded protuberances at the top (Fig. 2D). Looking at the height profiles, the height within multilayers increased in increments of the approximate thickness of the single bilayer, as determined in the samples containing only SP-B, being the mean value measured for these double bilayers of 12.9 ± 1.9 nm (n = 5). We therefore find here the combined effect of both proteins in the film conformation. SP-B helps with the association of bilayers but is not able to stabilize more than 2 bilayer stacks. This suggests that SP-B substantially improves surface activity by increasing lipid affinity and contributing to the formation of multi-layered structures that aid in re-spreading lipid material at the surface. SP-C on its side promotes the bending of the top layers at the surface of the membrane and reduces the surface tension between them. It has been shown that artificial or natural pulmonary surfactants that are functional (i.e. capable of reducing the surface tension to very low values) show characteristic patterns of multilayer stacks attached to the interfacial film. Various bilayer stacks, as those observed in LM with SP-B and SP-C, are likely required for the mechanical stability of the functional surfactant films. For the bilayer stacks to be mechanically reinforcing, they must be cross-linked to each other's. Otherwise, they will separate or glide over the surface and have no mechanical effect. The membrane organisation observed here suggests that SP-B is likely acting as the cross-linker between bilayers. The images also suggest that SP-C has to be present to stabilize high multilayer structures linked through SP-B. When measuring the height of the SLBs obtained with this sample, they resemble the one with only SP-C, with values of 6.63 ± 0.38 nm at 20 °C and 7.2 ± 0.3 nm at 37 °C.

Our results with synthetic films were compared with the images obtained from two different natural surfactant samples: native surfactant (NS), a whole pulmonary surfactant preparation purified from bronchoalveolar lavages of porcine lungs and amniotic fluid surfactant (AFS), purified from human amniotic fluid (Fig. 1 and Fig. 4). Although we observed differences in thickness (Fig. 1) that we interpret as due to their structural differences, some common topographical features for both systems can be observed (Fig. 4). In both cases we find a coexistence of large flat single bilayers and smaller size higher multilayers, which are densely packed with small protrusions of up to 50 nm in size. This could mean that multiple bilayers appear attached to the surface, although this cannot be unambiguously interpreted from the AFM data. Hence in general terms, the native systems show high complexity with lateral and vertical stability. This multilayer organization is similar to what we observed in the synthetic system containing both SP-B and SP-C. This highlights the importance of both proteins to complement the functional organization of the surfactant system.

3.1.1. *Young's modulus*

In a typical AFM nanoindentation experiment, the cantilever of the AFM is approached to the sample until the tip makes contact with it and the cantilever deflects upwards as the tip indents the sample. From the cantilever deflection vs. displacement curves it is possible to calculate the mechanical properties of the sample, such as the Young's Modulus E, using Sneddon's models (Sneddon, 1948). Fitting the indentation region in each of the extension curves with the Sneddon model yielded the Young's modulus values, and the distribution of these values for the supported bilayers formed by the different studied samples were grouped and plotted in Fig. 5. In order to obtain the Young's Modulus of the different bilayers, we fitted only the 2 nm depth of the indentation curve after the contact point, to minimize the effect of the hard mica support on the curve shape. An example of a fitted curve is given in the inset of Fig. 5A.

Fig. 5 summarizes and compares the Young's Modulus (E) histograms obtained from indentation experiments with the different systems tested. The Young modulus of protein-free LM exhibited a mean value of E_{LM} = 12.05 ± 0.8 MPa at 20 °C and E_{LM} = 10.85 ± 1.77 MPa at 37 °C, with a narrow distribution ranging from 7 to 15 MPa (Fig. 5A). The lowest values of the range correspond to the disordered phase, whereas ordered domains should be associated with less elastic deformation and a higher degree of compactness. In contrast, the mean Young modulus of the LM containing proteins SP-B or SP-C was significantly lower, with $E_{LM\text{-}SP\text{-}B}$ = 2.18 ± 0.59 MPa at 20 °C and $E_{LM\text{-}SP\text{-}B}$ = 2.90 ± 2 MPa at 37 °C, and $E_{LM\text{-}SP\text{-}C}$ = 5.3 ± 0.62 MPa at 20 °C and $E_{LM\text{-}SP\text{-}C}$ = 5.76 ± 1.6 MPa at 37 °C (Fig. 5B). The fact that bilayers containing proteins exhibited significantly lower Young modulus illustrates how protein incorporation modifies the structural organization of the lipid membrane. The E histograms for LM containing both SP-B and SP-C showed a broad range of Young modulus values from less than 1–10 MPa, covering the whole range of values measured for the LM membranes with SP-B and SP-C separately (Fig. 5C). That means that each protein

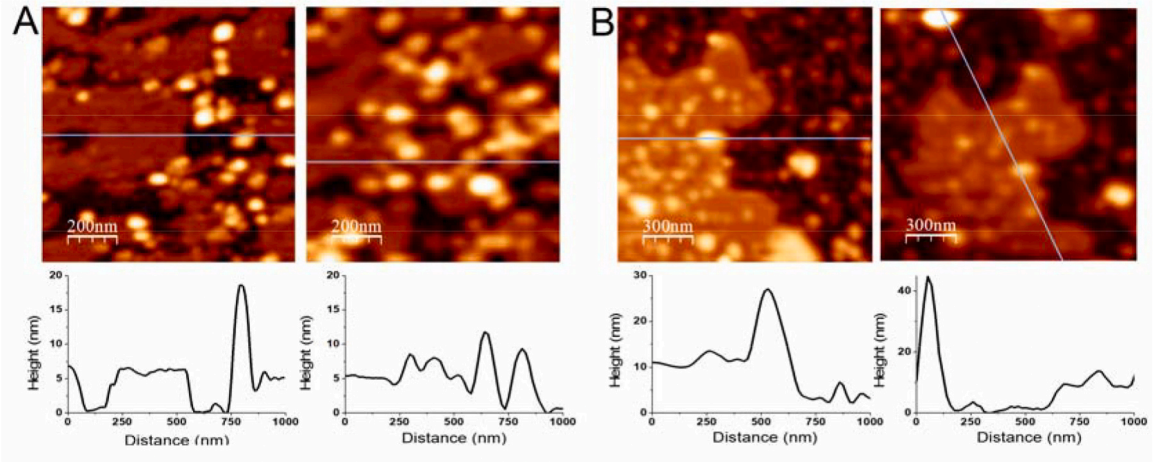

Fig. 4. Topographic AFM images and height profiles of supported membranes formed by whole natural surfactants obtained from bronchoalveolar porcine lavage or human amniotic fluid. Images in the figure cover 1 × 1 μm^2 (Z-scale: 30 nm) from (A) A native surfactant (NS) purified from bronchoalveolar lavage of porcine lungs and 1.5 × 1.5 μm^2 (Z-scale: 30 nm) from (B) an amniotic fluid surfactant (AFS) purified from human amniotic fluid. The images were obtained for each sample at both 20°C (left) and 37°C (right).

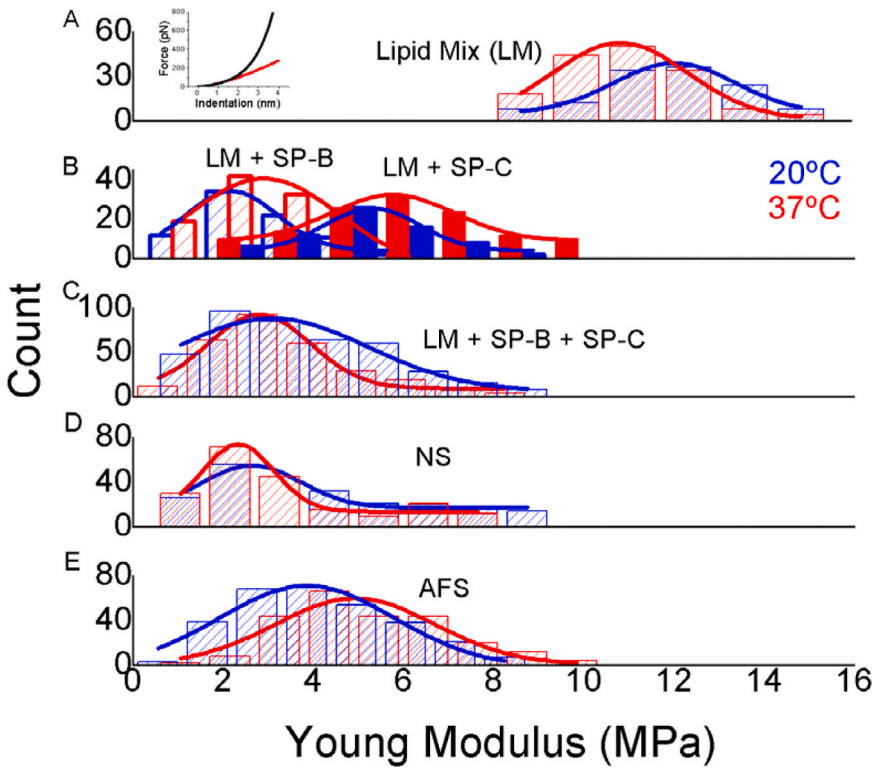

Fig. 5. Young modulus of lipid and lipid-protein supported surfactant membranes. The histograms of Young's Modulus values with Gaussian fittings are presented as calculated at 20 (blue) or 37 °C (red) for bilayers made of (A) the LM mixture, DPPC/POPC/POPG (50:25:15), (B) LM with 10 % SP-B and LM with 10 % SP-C, (C) LM with 10 % each of both proteins SP-B and SP-C, and the natural system purified from (D) bronchoalveolar lavages of porcine lungs (NS) and (E) human amniotic fluid (AFS). The inset on top left of Fig. 5A shows an example of indentation curve (black) with the Sneddon model fitting (red) onto the first 2 nm of indentation within the LM membrane.

might contribute significantly to the heterogeneous elasticity distribution in LM membranes.

The whole natural surfactant systems analysed showed similar elastic response. For both NS and AFS samples the elastic response measured is broad, with a value for NS of $E_{NS} = 2.64 \pm 1.48$ MPa at 20 °C and $E_{NS} = 2.3 \pm 1.48$ MPa at 37 °C and for AFS of $E_{AFS} = 3.86 \pm 1.13$ MPa at 20 °C and $E_{AFS} = 4.92 \pm 2.07$ MPa at 37 °C (Fig. 5D and E). Such heterogeneity in the E value is likely a consequence of the compositional anisotropy of the films, which somehow facilitates lipid motion and transfer during compression and re-spreading.

These results illustrate how AFM imaging coupled with indentation measurements provides direct correlation of the organization of multi-component lipid mixtures to their nanomechanical properties, to extents that were not previously achieved. We can directly correlate the presence of proteins integrated into the membranes with their stability once subjected to mechanical stress and potentially deforming forces. LM membranes with SP-B and SP-C incorporated become closer to natural surfactants and possess similar elastic properties among other features. This validates the use of this type of synthetic system to mimic in a simplified manner the behaviour of natural membranes.

4. Discussion

In this work we have used SLBs as models for surfactant bilayers and multilayers, in an attempt to decouple the contribution of membrane resistance to deformation in the possible performance of the complex interfacial layers formed by surfactant at the alveolar spaces, including the possible effects of membrane/membrane interactions promoted by the proteins. The relevance of the study is reinforced by the comparison of the behavior of model materials with the supported layers formed by two native preparations of different origin, which could represent different physiological scenarios of surfactant before and after being subjected to respiratory work at the pulmonary air-exposed surface.

Surfactant-mimicking pure phospholipid vesicles spontaneously form flat supported lipid bilayers (Fig. 2), while samples containing proteins originated different structures onto the mica surface beyond SLBs. Samples containing SP-B spread to form much larger membranes than samples with no SP-B (Fig. 2**B**), which could be connected with the ability of SP-B to promote vesicle aggregation, membrane-membrane contacts and transfer of lipids from one layer to another (Pérez-Gil, 2008; Olmeda et al., 2015; Baoukina and Tieleman, 2010; Parra et al., 2011, 2013). These activities of SP-B are likely also behind the formation of multi-layered structures, detected as a coexistence of membranes with an approximate thickness of 6 nm and 12 nm. Interestingly, we did not observe thicker stacks of membranes, which could be related to a potential enrichment of the protein at the region of contact between the first two bilayers, which would lead to no more protein available to attach other membranes (Cabré et al., 2009). In contrast, the samples containing only SP-C showed many associated vesicles of small size, not fully spread on the mica (Fig. 3), supporting the reported ability of this protein to promote membrane budding and vesicle fragmentation (Roldan et al., 2016). Still, once the SLB is formed, synthetic membranes containing SP-C appeared thicker, as illustrated in Fig.1. This could be an effect associated with the transmembrane orientation of the protein within the bilayer (Roldan et al., 2015; Plasencia et al., 2008).

The system in which containing both hydrophobic proteins exhibited large membranes composed of multiple bilayers with some of them not fully spread (Fig. 2D). This could indicate a cooperation of the two proteins to combine the flexibility effect provided by SP-C and the aggregation ability of SP-B to facilitate the formation of multi-layered stacks (Parra et al., 2011; Schürch et al., 2010). These complementary effects should affect membrane mechanical properties, which may be relevant for the physiological performance of interfacial films with tightly associated membranes (Pérez-Gil, 2008; Yu and Possmayer,

2003; Cabré et al., 2018; Parra et al., 2011, 2013; Amrein et al., 1997; Taneva and Keough, 1994; Baumgart et al., 2010; Serrano and Pérez-Gil, 2006).

It is remarkable that the two natural systems studied, the native surfactant (NS) isolated from bronchoalveolar lavages and the human amniotic fluid surfactant (AFS) representing a freshly secreted surfactant still unexposed to air, had the capability to spread efficiently as they were purified from natural environments, both at 20 °C and 37 °C. Taking into account the different timescale, geometry, and mechanism by which the adsorption process could occur *in vivo* and *in vitro* (Plunkett et al., 2013), the fact of having more surface covered by the natural materials indicates that they are working better in terms of adsorption and spreading onto the surface than the materials artificially prepared.

As it could be somehow expected, fully complex native surfactant samples look highly heterogeneous, making more difficult to perform conclusive quantitative measurements. In the topographic images, large membranes with different heights and a high number of particles around them are observed. Those structures could be somehow analogous to those formed when newly secreted surfactant arrives to the outer surface of bilayer structures associated to already adsorbed surfactant films. Still, it is worth mentioning that the polar and highly charged mica surface is by no means comparable to the air-liquid interface at the alveolar spaces, preventing a complete extrapolation to the *in vivo* behaviour of these native materials (Pérez-Gil, 2008; Lopez-Rodriguez and Pérez-Gil, 2014; Castillo-Sánchez et al., 2022, 2021).

From the information provided by the Young's modulus, we can deduce that the incorporation of the proteins introduces significant structural changes into the bilayers. These changes in E could help to explain the biophysical importance of proteins to modulate surfactant membrane mechanics. The values determined here for E, upon vertical deformation introduced by indentation of the AFM cantilever in a direction perpendicular to the plane of the supported membranes, have at least two components that can be of relevance for the behaviour of surfactant membranes in the alveolar scenario. First, it introduces a lateral compressive contribution as the tip gets deep into the core of the bilayers. The relative resistance of the film to such lateral compressive wave may somehow reflect, at least in part, the response of interfacial surfactant layers during exhalation, when the reduction in lung volume forces a net reduction in the surface area available. High lateral pressure presumably defines the ability of the surfactant films to collapse when they are at the air-liquid interface, in a process that has been extensively analysed (Lhert et al., 2007; Yan et al., 2005). A second component in the indentation experiment is the net vertical force applied perpendicularly to the lipid layers, which may therefore also induce the lipid layers to respond by breaking or collapsing out-of-plane (Pocivavsek et al., 2008). These forces may be representative of the mechanical forces actually occurring at the alveolar spaces during the breathing cycle, when different regions of the lungs change their volume in a non-synchronous way, or when the respiratory surface film is subjected to shocking waves caused by movement, cough, sneezing, etc. It is also worth mentioning that, contrary to what happens with the LM, the E parameter slightly increases as a function of temperature when SP-B or SP-C are included in the sample by their own, what also informs about the ability of the proteins to affect lipid packing and organization. Although no significant differences are observed in any case as a matter of temperature, AFS membranes also seem to be more ordered at 37 °C as they present higher E values than measured at 20 °C, what could have to do with their densely packed structure (Castillo-Sánchez et al., 2022).

We propose that the Young's modulus measured in surfactant (multi) bilayers as a response to vertical deformation forces could depend on at least 4 different factors. A first factor would be lateral in-plane molecular diffusion and the ability of surfactant membranes to "dissipate" a transient reduction in available area. In this sense, surfactant proteins SP-B and SP-C have been reported to modulate lateral phospholipid diffusion (Bernardino de la Serna et al., 2009; Liekkinen et al., 2023). A second factor could be membrane thickness, which may influence the resistance to breakage of each single bilayer within complex multilayer films. Many antimicrobial peptides that end breaking their target membranes produce at first instance a thinning of the bilayers that makes them more susceptible to rupture (Agadi et al., 2022). Our results indicate that both SP-B and SP-C increase the thickness of surfactant membranes, especially as a consequence of the presence of the rigid transmembrane helix of SP-C (Roldan et al., 2015). A third important factor would be the protein-promoted stabilization of highly cohesive multilayer configurations, particularly due to the membrane-membrane interacting properties of SP-B (Bernardino de la Serna et al., 2013a). Finally, a last factor could be related with the ability of SP-B to facilitate the rapid movement of phospholipids between membranes (Liekkinen et al., 2020a). The particularly low E values of membranes containing SP-B could be at least in part due to the relaxation of transient pressures via the movement of the more fluid lipids through the intermembrane lipid channels assembled by SP-B oligomers (Olmeda et al., 2015).

The combined action of SP-B and SP-C could then optimize the mechanical resistance of surfactant layers through a variable contribution of both proteins to these different factors. With both proteins together into the lipid mixture, the E histogram resembles a mixture of the entire range of values described for either protein separately. We would like to remark that our simplified model composed of DPPC/POPC/POPG + SP-B + SP-C mimics quite adequately the natural systems in terms of elasticity, as seen in the histograms of Fig. 5. The mechanical properties of the natural surfactant complexes studied here result to be particularly prone to extend and form membrane-based structures associated to the mica supports (even at non-physiological temperatures), as well as they are presumably optimized to spread at air-liquid interfaces. It is important to consider that natural samples also contain the membrane-associated collectin SP-A, as well as cholesterol, which is able to modulate the segregation of lipids in lateral structures (Bernardino de la Serna et al., 2009, 2004, 2013b; Liekkinen et al., 2020b). This could be the reason why broader E histograms are obtained for natural samples. The presence of cholesterol could also account for at least part of the differences in morphology observed between synthetic and natural samples. No cholesterol has been included into our simplified lipid models as it is usually depleted from clinical surfactant to avoid reported inhibitory actions of abnormal proportions of cholesterol into the surface activity of PS (Echaide et al., 2017). Nevertheless, further studies are guaranteed to establish the importance of cholesterol in the mechanical properties of PS, especially in the presence of SP-C (Gómez-Gil et al., 2009).

We are aware that our study has some limitations that should be taken into account before extrapolating some conclusions to the physiological context. The effect of proteins in the mechanical properties of SLBs could be better assessed upon comparison of the behaviour of systems with different protein amounts. Here, we wanted to populate the membrane regions where the proteins are present to detect clear effects that could still occur at lower, physiological, protein contents at least in defined regions of PS membranes and films. The comparison with the native materials, in which the proteins are found in physiological proportions, is a good reference to recognize the specific effects of the proteins that we observe better in the study of simplified model samples. Another limitation is that we have not considered some factors that could be important in the alveolar context. For instance, the presence of millimolar calcium concentrations could have a significant contribution in the mechanical resistance of PS membranes and films. We did not include calcium in our study to avoid the possible contribution of ionic interactions of this cation with surfactant membranes at the mica surface, where it is known to promote membrane adhesiveness in ways that would not represent a true pulmonary context. Finally, despite the advantages of using SLBs in mechanical studies under AFM, it is clear that they can be far from the study of the behaviour of analogous materials once associated to air-liquid interfaces. Still, we are still persuaded that the results obtained here could be informing about the effect of proteins in the locations in which multi-layered membrane

arrays would be formed.

CRediT authorship contribution statement

Antonio Cruz: Writing – review & editing, Supervision, Conceptualization. **Jesus Perez-Gil:** Writing – review & editing, Supervision, Project administration, Funding acquisition, Conceptualization. **Johann Mertens:** Writing – review & editing, Validation, Methodology, Investigation, Formal analysis. **Emma Batllori-Badia:** Resources. **Ainhoa Collada:** Writing – review & editing, Writing – original draft, Investigation, Formal analysis. **Alberto Galindo:** Resources.

Declaration of Competing Interest

The authors declare the following financial interests/personal relationships which may be considered as potential competing interests: Editor-in-Chief of Chemistry and Physics of Lipids - J.P.-G. If there are other authors, they declare that they have no known competing financial interests or personal relationships that could have appeared to influence the work reported in this paper.

Acknowledgements

This research has been funded by grants from the Spanish Ministry of Science and Innovation (PID2021-124932OB-100, PGC2018-099713-B-100), and the Regional Government of Madrid (P2018/NMT-4389).

Data Availability

Data will be made available on request.

References

Pérez-Gil, J., 2008. Structure of pulmonary surfactant membranes and films: the role of proteins and lipid-protein interactions. Biochim Biophys. Acta 1778 (7-8), 1676–1695.
Echaide, M., et al., 2017. Restoring pulmonary surfactant membranes and films at the respiratory surface. Biochim Biophys. Acta Biomembr. 1859 (9 Pt B), 1725–1739.
Haller, T., et al., 2004. Tracing surfactant transformation from cellular release to insertion into an air-liquid interface. Am. J. Physiol. Lung Cell Mol. Physiol. 286 (5), L1009–L1015.
Veldhuizen, R., et al., 1998. The role of lipids in pulmonary surfactant. Biochim Biophys. Acta 1408 (2-3), 90–108.
Yu, S.H., Possmayer, F., 2003. Lipid compositional analysis of pulmonary surfactant monolayers and monolayer-associated reservoirs. J. Lipid Res 44 (3), 621–629.
Lopez-Rodriguez, E., Pérez-Gil, J., 2014. Structure-function relationships in pulmonary surfactant membranes: from biophysics to therapy. Biochim Biophys. Acta 1838 (6), 1568–1585.
Melton, K.R., et al., 2003. SP-B deficiency causes respiratory failure in adult mice. Am. J. Physiol. Lung Cell Mol. Physiol. 285 (3), L543–L549.
Olmeda, B., et al., 2015. A model for the structure and mechanism of action of pulmonary surfactant protein B. Faseb J. 29 (10), 4236–4247.
Baoukina, S., Tieleman, D.P., 2011. Lung surfactant protein SP-B promotes formation of bilayer reservoirs from monolayer and lipid transfer between the interface and subphase. Biophys. J. 100 (7), 1678–1687.
Baoukina, S., Tieleman, D.P., 2010. Direct simulation of protein-mediated vesicle fusion: lung surfactant protein B. Biophys. J. 99 (7), 2134–2142.
Keating, E., et al., 2012. A modified squeeze-out mechanism for generating high surface pressures with pulmonary surfactant. Biochim Biophys. Acta 1818 (5), 1225–1234.
Roldan, N., et al., 2015. Palmitoylation as a key factor to modulate SP-C-lipid interactions in lung surfactant membrane multilayers. Biochim Biophys. Acta 1848 (1 Pt A), 184–191.
Plasencia, I., et al., 2008. Effect of acylation on the interaction of the N-Terminal segment of pulmonary surfactant protein SP-C with phospholipid membranes. Biochim Biophys. Acta 1778 (5), 1274–1282.
Takamoto, D.Y., et al., 2001. Interaction of lung surfactant proteins with anionic phospholipids. Biophys. J. 81 (1), 153–169.
Cabré, E.J., et al., 2018. Homo- and hetero-oligomerization of hydrophobic pulmonary surfactant proteins SP-B and SP-C in surfactant phospholipid membranes. J. Biol. Chem. 293 (24), 9399–9411.
Parra, E., et al., 2011. A combined action of pulmonary surfactant proteins SP-B and SP-C modulates permeability and dynamics of phospholipid membranes. Biochem J. 438 (3), 555–564.
Pfister, R.H., Soll, R., Wiswell, T.E., 2009. Protein-containing synthetic surfactant versus protein-free synthetic surfactant for the prevention and treatment of respiratory distress syndrome. Cochrane Database Syst. Rev. Cd006180, 4.
Singh, N., et al., 2015. Comparison of animal-derived surfactants for the prevention and treatment of respiratory distress syndrome in preterm infants. Cochrane Database Syst. Rev. 2015 (12), Cd010249.
Castillo-Sánchez, J.C., et al., 2022. The highly packed and dehydrated structure of preformed unexposed human pulmonary surfactant isolated from amniotic fluid. Am. J. Physiol. Lung Cell Mol. Physiol. 322 (2), L191 l203.
Hallman, M., et al., 1983. Isolation of human surfactant from amniotic fluid and a pilot study of its efficacy in respiratory distress syndrome. Pediatrics 71 (4), 473–482.
Hallman, M., et al., 1976. Phosphatidylinositol and phosphatidylglycerol in amniotic fluid: indices of lung maturity. Am. J. Obstet. Gynecol. 125 (5), 613–617.
Lemke, A., et al., 2017. Human amniotic membrane as newly identified source of amniotic fluid pulmonary surfactant. Sci. Rep. 7 (1), 6406.
Pérez-Gil, J., Cruz, A., Casals, C., 1993. Solubility of hydrophobic surfactant proteins in organic solvent/water mixtures. Structural studies on SP-B and SP-C in aqueous organic solvents and lipids. Biochim Biophys. Acta 1168 (3), 261–270.
Taeusch, H.W., et al., 2005. Inactivation of pulmonary surfactant due to serum-inhibited adsorption and reversal by hydrophilic polymers: experimental. Biophys. J. 89 (3), 1769–1779.
Sneddon, I.N., 1948. Boussinesq's problem for a rigid cone. Math. Proc. Camb. Philos. Soc. 44, 492–507.
Horcas, I., et al., 2007. WSXM: a software for scanning probe microscopy and a tool for nanotechnology. Rev. Sci. Instrum. 78 (1), 013705.
Hermanowicz, P., et al., 2014. AtomicJ: an open source software for analysis of force curves. Rev. Sci. Instrum. 85 (6), 063703.
Parra, E., et al., 2013. Hydrophobic pulmonary surfactant proteins SP-B and SP-C induce pore formation in planar lipid membranes: evidence for proteolipid pores. Biophys. J. 104 (1), 146–155.
Cabré, E.J., et al., 2009. Surfactant protein SP-B strongly modifies surface collapse of phospholipid vesicles: insights from a quartz crystal microbalance with dissipation. Biophys. J. 97 (3), 768–776.
Roldan, N., et al., 2016. Effect of Lung Surfactant Protein SP-C and SP-C-promoted membrane fragmentation on cholesterol dynamics. Biophys. J. 111 (8), 1703–1713.
Schürch, D., et al., 2010. Combined and independent action of proteins SP-B and SP-C in the surface behavior and mechanical stability of pulmonary surfactant films. Biophys. J. 99 (10), 3290–3299.
Amrein, M., von Nahmen, A., Sieber, M., 1997. A scanning force- and fluorescence light microscopy study of the structure and function of a model pulmonary surfactant. Eur. Biophys. J. 26 (5), 349–357.
Taneva, S., Keough, K.M., 1994. Pulmonary surfactant proteins SP-B and SP-C in spread monolayers at the air-water interface: II. Monolayers of pulmonary surfactant protein SP-C and phospholipids. Biophys. J. 66 (4), 1149–1157.
Baumgart, F., et al., 2010. Palmitoylation of pulmonary surfactant protein SP-C is critical for its functional cooperation with SP-B to sustain compression/expansion dynamics in cholesterol-containing surfactant films. Biophys. J. 99 (10), 3234–3243.
Serrano, A.G., Pérez-Gil, J., 2006. Protein-lipid interactions and surface activity in the pulmonary surfactant system. Chem. Phys. Lipids 141 (1-2), 105–118.
Plunkett, P., et al., 2013. Simulation of edge facilitated adsorption and critical concentration induced rupture of vesicles at a surface. Soft Matter 9 (35), 8420.
Castillo-Sánchez, J.C., Cruz, A., Pérez-Gil, J., 2021. Structural hallmarks of lung surfactant: Lipid-protein interactions, membrane structure and future challenges. Arch. Biochem Biophys. 703, 108850.
Lhert, F., et al., 2007. Effects of hydrophobic surfactant proteins on collapse of pulmonary surfactant monolayers. Biophys. J. 93 (12), 4237–4243.
Yan, W., Piknova, B., Hall, S.B., 2005. The collapse of monolayers containing pulmonary surfactant phospholipids is kinetically determined. Biophys. J. 89 (1), 306–314.
Pocivavsek, L., et al., 2008. Lateral stress relaxation and collapse in lipid monolayers. Soft Matter 4, 2019–2029.
Bernardino de la Serna, J., et al., 2009. Segregated phases in pulmonary surfactant membranes do not show coexistence of lipid populations with differentiated dynamic properties. Biophys. J. 97 (5), 1381–1389.
Liekkinen, J., et al., 2023. Surfactant Proteins SP-B and SP-C in pulmonary surfactant monolayers: physical properties controlled by specific protein-lipid interactions. Langmuir 39 (12), 4338–4350.
Agadi, N., et al., 2022. Distinct mode of membrane interaction and disintegration by diverse class of antimicrobial peptides. Biochim Biophys. Acta Biomembr. 1864 (12), 184047.
Bernardino de la Serna, J., et al., 2013a. Segregated ordered lipid phases and protein-promoted membrane cohesivity are required for pulmonary surfactant films to stabilize and protect the respiratory surface. Faraday Discuss. 161, 535–548 discussion 563-89.
Liekkinen, J., et al., 2020a. Pulmonary surfactant lipid reorganization induced by the adsorption of the oligomeric surfactant protein B complex. J. Mol. Biol. 432 (10), 3251–3268.
Bernardino de la Serna, J., et al., 2004. Cholesterol rules: direct observation of the coexistence of two fluid phases in native pulmonary surfactant membranes at physiological temperatures. J. Biol. Chem. 279 (39), 40715–40722.
Bernardino de la Serna, J., et al., 2013b. Compositional and structural characterization of monolayers and bilayers composed of native pulmonary surfactant from wild type mice. Biochim Biophys. Acta 1828 (11), 2450–2459.
Liekkinen, J., et al., 2020b. Understanding the functional properties of lipid heterogeneity in pulmonary surfactant monolayers at the atomistic level. Front Cell Dev. Biol. 8, 581016.
Gómez-Gil, L., Pérez-Gil, J., Goormaghtigh, E., 2009. Cholesterol modulates the exposure and orientation of pulmonary surfactant protein SP-C in model surfactant membranes. Biochim Biophys. Acta 1788 (9), 1907–1915.